Molecular Biology of the Cell
Vol. 18, 1497–1506, April 2007

Fatty Acid Remodeling of GPI-anchored Proteins Is Required for Their Raft Association[D]

Yusuke Maeda,* Yuko Tashima,* Toshiaki Houjou,† Morihisa Fujita,‡ Takehiko Yoko-o,‡ Yoshifumi Jigami,‡ Ryo Taguchi,† and Taroh Kinoshita*

*Research Institute for Microbial Diseases, Osaka University, Osaka 565-0871, Japan; †Graduate School of Medicine, University of Tokyo, Bunkyoku, Tokyo 113-0033, Japan; and ‡Research Center for Glycoscience, National Institute of Advanced Industrial Science and Technology, Tsukuba, Ibaraki 305-8566, Japan

Submitted October 2, 2006; Revised January 26, 2007; Accepted February 1, 2007
Monitoring Editor: Reid Gilmore

Whereas most of the cellular phosphatidylinositol (PI) contain unsaturated fatty chains and are excluded from rafts, GPI-anchored proteins (APs) unusually contain two saturated fatty chains in their PI moiety, and they are typically found within lipid rafts. However, the origin of the saturated chains and whether they are essential for raft association are unclear. Here, we report that GPI-APs, with two saturated fatty chains, are generated from those bearing an unsaturated chain by fatty acid remodeling that occurs most likely in the Golgi and requires post-GPI-attachment to proteins (PGAP)2 and PGAP3. The surface GPI-APs isolated from the PGAP2 and -3 double-mutant Chinese hamster ovary (CHO) cells had unsaturated chains, such as oleic, arachidonic, and docosatetraenoic acids in the sn-2 position, whereas those from wild-type CHO cells had exclusively stearic acid, a saturated chain, indicating that the sn-2 chain is exchanged to a saturated chain. We then assessed the association of GPI-APs with lipid rafts. Recovery of unremodeled GPI-APs from the double-mutant cells in the detergent-resistant membrane fraction was very low, indicating that GPI-APs become competent to be incorporated into lipid rafts by PGAP3- and PGAP2-mediated fatty acid remodeling. We also show that the remodeling requires the preceding PGAP1-mediated deacylation from inositol of GPI-APs in the endoplasmic reticulum.

INTRODUCTION

GPI is a glycolipid widely found among eukaryotes that anchors many proteins to the outer leaflet of the plasma membrane (McConville and Ferguson, 1993; Ferguson, 1999; Ikezawa, 2002). The carboxy termini of precursor proteins are processed and covalently attached with GPI in the endoplasmic reticulum (ER), resulting in GPI-anchored proteins (APs). The common core structure of GPI is conserved among all species. GPI-APs are transported to the plasma membrane, and they are associated with lipid rafts, consisting mainly of sphingolipids and cholesterol (Simons and Ikonen, 1997), although there is still some controversy about the definition and existence of physiologically relevant lipid rafts (Simons and Toomre, 2000; Hancock, 2006). The lipid rafts modulate various biological functions of GPI-APs, such as signal transduction, endocytosis, and apical sorting (Brown and Rose, 1992; Harder and Simons, 1997; Tansey *et al*., 2000; Ikezawa, 2002; Sabharanjak *et al*., 2002; Paladino *et al*., 2004); therefore, the raft association is important to understand their functions. GPI is thought to be a strong determinant for the integration of GPI-APs into rafts (Harder and Simons, 1997), and if GPI is replaced with transmembrane region of other nonraft protein, in most cases proteins lose their abilities to be associated with rafts (Tansey *et al*., 2000; Marquardt *et al*., 2005). Whereas most of the cellular phosphatidylinositol (PI) contains unsaturated fatty chains at sn-2 position (Kerwin *et al*., 1994), the PI moiety of mammalian GPI-APs consists mainly of saturated chains (McConville and Ferguson, 1993; Redman *et al*., 1994; Brewis *et al*., 1995; Treumann *et al*., 1995; Benting *et al*., 1999), although GPI-APs with unsaturated fatty chain at sn-2 position were also reported on some cells and molecules (Roberts *et al*., 1988; Wong and Low, 1992; Redman *et al*., 1994; Treumann *et al*., 1995). The saturated fatty chains in GPI are implied in the association with the liquid-ordered raft membrane by analogy of other phospholipids (Schroeder *et al*., 1994; Raza Shaikh *et al*., 2003) and palmitoylated proteins (Melkonian *et al*., 1999; Moffett *et al*., 2000; Zhang *et al*., 2000). However, the origin of saturated chains in GPI is unclear along with whether they are essential for raft association.

One idea to explain how saturated chains in mammalian GPI are synthesized is that GPI may use lipid remodeling. In lower microorganisms, processing of lipid moieties of GPI, called lipid remodeling, is well known, but the physiological significance is still an outstanding issue. In *Saccharomyces cerevisiae*, sn-2–linked acyl chain in PI moiety is changed to C26:0 chain and/or diacylglycerol moiety is replaced with ceramide after GPI is transferred to proteins and inositol-linked palmitic acid is removed (Sipos *et al*., 1997; Bosson *et al*., 2006). Bloodstream form of *Trypanosoma brucei*, a causative agent of African sleeping sickness, exchanges both acyl

This article was published online ahead of print in *MBC in Press* (http://www.molbiolcell.org/cgi/doi/10.1091/mbc.E06–10–0885) on February 21, 2007.

[D] The online version of this article contains supplemental material at *MBC Online* (http://www.molbiolcell.org).

Address correspondence to: Taroh Kinoshita (tkinoshi@biken.osaka-u.ac.jp).

Abbreviations used: AP, anchored protein; CHO, Chinese hamster ovary; DAF, decay accelerating factor; DRM, detergent-resistant membrane; ER, endoplasmic reticulum; PGAP, post-GPI-attachment to proteins; PI, phosphatidylinositol; PLA, phospholipase A.

chains in PI of GPI strictly to myristate (C14:0) in the ER before attachment of GPI to variant surface glycoproteins (Morita *et al*., 2000). In contrast, very little is known so far in mammalian cells except for the presence of deacylation of inositol-linked acyl chain after conjugation of GPI with proteins in the ER. We previously reported Chinese hamster ovary (CHO) cells with defects in Golgi/ER-resident post-GPI-attachment to proteins (PGAP)2 (Tashima *et al*., 2006). In PGAP2-deficient CHO cells, the surface expression of GPI-APs was decreased owing to rapid secretion of cleaved GPI-APs into the culture medium. We found that two sequential cleavages of GPI took place in the Golgi and cell surface in PGAP2-deficient CHO cells (Tashima *et al*., 2006). First, GPI-APs were converted to lyso-GPI-APs by phospholipase A (PLA) activity by the time when newly synthesized GPI-APs exit from the *trans*-Golgi network. Second, this event was followed by cleavage of lyso-GPI-APs by phospholipase D (PLD) activity on the cell surface, resulting in secretion of GPI-APs. Although we have not identified the surface PLD yet, it seemed different from GPI-PLD, a well-known PLD abundant in serum, and might be specific for lyso-form GPI-APs because normal GPI-APs carrying two lipid chains are resistant to this PLD activity. We hypothesized that lyso-GPI-AP was an intermediate in the process of fatty acid remodeling, which ought to be reacylated with a saturated chain in the presence of PGAP2. We expected that if the PLA activity involved in the fatty acid remodeling is lost in PGAP2-deficient cells, GPI-APs would remain unremodeled and have two lipid chains as normal GPI-APs, resulting in recovery of the surface expressions due to the resistant to the surface PLD. To prove our hypothesis, here we report establishment and characterization of double-mutant cells from PGAP2-deficient CHO cells, in which surface expression of GPI-APs was indeed restored, and we reveal the significance of fatty acid remodeling on the raft association of GPI-APs.

MATERIALS AND METHODS

Cells, Antibodies, and Materials

All cell lines used in this study were derivatives of CHO cells, and they are summarized in Table 1. Wild-type 3B2A and GD3S-C37, PGAP2-deficient C84 and AM-B (Tashima *et al*., 2006), and PGAP1-deficient C10 (Tanaka *et al*., 2004) cells were described previously. All cell lines were cultured in Ham's F-12 medium (Sigma-Aldrich, St. Louis, MO) supplemented with 10% fetal calf serum and 600 μg/ml Geneticin (G-418; Invitrogen, Carlsbad, CA) with various combinations of 6 μg/ml puromycin, 600 μg/ml hygromycin, 6 μg/ml blasticidin, and 250 μg/ml zeocin for maintenance of transfected plasmids. 3B2A and DM2&3-C2 cells stably expressing HFGF-CD59 were established by transfection of linealized pME-pgkpuro-HFGF-CD59 and pME-pgkhyg-HFGF-CD59, respectively. After selection with antibiotics, cells expressing high levels of HFGF-CD59 were sorted in FACS Vantage (BD Biosciences, San Jose, CA) after staining with anti-FLAG antibody and limiting-diluted to obtain clones. DM2&3-C2 cells restored with PGAP2 and PGAP3 were established under the selection with zeocin by transient expression of mCAT1, a receptor for ecotropic retroviruses, by using pME-KmCAT1 (a gift from Dr. K. Ohishi, Osaka University, Osaka, Japan), followed by infection of retrovirus that was produced in PLAT-E packaging cells (a gift from Dr. T. Kitamura, University of Tokyo, Tokyo, Japan) transfected with pMSCV-rPGAP2-zeo-hPGAP3.

The commercial antibodies used here were mouse monoclonal antibodies against transferrin receptor (Zymed Laboratories. South San Francisco, CA), caveolin1, flotillin1 and syntaxin6 (BD Biosciences), FLAG-tag (clone M2; Sigma-Aldrich) and hemagglutinin-tag (clone HA7; Sigma-Aldrich) and rabbit polyclonal antibodies against GPP130 (Covance, Princeton, NJ) and goat polyclonal antibody against ribophorin II (Santa Cruz Biotechnology, Santa Cruz, CA). Secondary antibodies used were horseradish peroxidase (HRP)-conjugated anti-mouse IgG, anti-rabbit IgG (GE Healthcare, Little Chalfont, Buckinghamshire, United Kingdom), and anti-goat IgG (Promega, Madison, WI), phycoerythrin (PE)-conjugated goat anti-mouse IgG (BD Biosciences PharMingen, San Diego, CA), and Alexa488-conjugated goat anti-mouse IgG and Alexa594-conjugated goat anti-rabbit IgG (Invitrogen). Mouse IgG1 monoclonal antibody against hamster urokinase-type plasminogen activator receptor (uPAR) (clone 5D6) was made in this laboratory by immunizing detergent-resistant membrane fractions obtained from CHO cells and by conventional method. The reactive protein to this antibody was purified by antibody-coupled affinity column by using Affi-Gel Hz (Bio-Rad, Hercules, CA), sequenced by tandem mass spectrometry (MS/MS), and identified as hamster uPAR. Mouse monoclonal antibodies against decay accelerating factor (DAF) (clone IA10) and CD59 (clone 5H8) were described previously (Tashima *et al*., 2006). Phosphatidylinositol-specific phospholipase C (PI-PLC) was purchased from Invitrogen.

Plasmid Construction

The expression vector of human PGAP3/PERLD1, constructed in pCMV·SPORT6, was purchased from Mammalian Gene Collection (clone ID 3855206; National Center for Biotechnology Information accession no. BC010652). Yeast PER1, amplified by polymerase chain reaction (PCR) (primers CTCCGTCGACCATGAGGTTAGCTGTGGTTGTGAC and GTGCTGCGGCCGCTAGTACAATTGTCTATTACCCCAATAGG) from pRS316T-PER1 (Fujita *et al*., 2006a), was subcloned into SalI and NotI sites of pCMV·SPORT6 vector. pME-hPGAP3/PERLD1-3HA, which expresses hPGAP3 carboxy-terminally tagged with three hemagglutinin (HA)-tags, was constructed by subcloning hPGAP3 amplified by PCR (primers GTGTACGGTGGGAGGTCTAT and GCTGACGCGTGTCCAGCTTGAACTTGTCCTCT) into EcoRI and MluI sites of pME-3HA vector (a gift from Dr. K. Ohishi). All fragments obtained by PCR were confirmed by sequencing. pMSCV-rPGAP2-zeo-hPGAP3 was constructed by ligation of EcoRI–XbaI fragment of rat PGAP2 from pME-PyrPGAP2 (Tashima *et al*., 2006), XbaI–BstZ17I fragment of SV40-zeo from pcDNA3.1-zeo (Invitrogen), and SspI–BamHI fragment of CMV-hPGAP3 from pCMV·SPORT6-hPGAP3 and EcoRI–BamHI vector portion of pMSCV-neo (Clontech, Mountain View, CA). pME-pgkpuro-HFGF-CD59 and pME-pgkhyg-HFGF-CD59 were constructed by subcloning EcoRI–NotI fragment of HFGF-CD59 into pME-pgkpuro and pME-pgkhyg (gifts from Dr. K. Ohishi), respectively.

Table 1. CHO cell lines used in this study

Cells	Parent cells	Derivation	Phenotype	Reference
CHO-K1			Wild type	
3B2A	CHO-K1	Stably expressing CD59 and DAF	Wild type	Tanaka *et al.* (2004)
C10	3B2A	Treated with EMS	*PGAP1*-deficient	Tanaka *et al.* (2004)
GD3S-C37	3B2A	Stably expressing GD3 synthase (and GD3 as the result)	Wild type	Tashima *et al.* (2006)
C84	GD3S-C37	Treated with EMS	*PGAP2*-deficient	Tashima *et al.* (2006)
DM2&3-C2	C84	Treated with EMS	*PGAP2&3*-deficient	This study
DM1&2-C17	C84	Treated with EMS	*PGAP1&2*-deficient	This study
F21.3.8.10	CHO-K1	Stably expressing CD59, DAF and many PIG genes involved in GPI biosynthesis	Wild type	Tashima *et al.* (2006)
AM-B	F21.3.8.10	Treated with EMS	*PGAP2*-deficient	Tashima *et al.* (2006)
DM1&2-C14	AM-B	Treated with EMS	*PGAP1&2*-deficient	This study

Cloning of Chinese Hamster PGAP3

A partial cDNA of hamster PGAP3 was obtained from CHO cDNA library by nested PCR with two degenerated primer sets of de1U (5′-CARTTYCAY-GGNAARTGGCCNTT-3′) and de4L (5′-ARRTANARNSWRTCRTCYTC-3′), and de2U (5′-TTYCAYACNMGNGAYACNGA-3′) and de3L (5′-ATRTGC-CADATNGCRTGNGCRTC-3′). Based on the sequence of obtained partial hamster PGAP3 cDNA, several new primers were designed, and PCRs with these primers and those corresponding to vector portion were done to obtained longer cDNA containing full coding region.

Analysis of PGAP3 mRNA by Sequencing and Real-Time Reverse Transcription (RT)-PCR

Total RNAs were obtained from GD3S-C37 (wild-type cells) and DM2&3-C2 (double-mutant cells) by using TRIzol (Invitrogen). First strand cDNAs were synthesized by PrimeScript RTase (Takara, Kyoto, Japan) with mixture of oligo(dT) and random primers as manufacturer's protocol. Real-time PCR was performed with SYBR Premix EX Taq (Takara) and Prism 7900HT (Applied Biosystems, Foster City, CA). Two sets of primer, set A (5′-ACTGAAG-CACTTCCGCTCCCT-3′ and 5′-GGCAGAAGCTGGCTCTTGGAT-3′ and set B (5′-CACATCAGCACCATTCCAGTC-3′ and 5′-AGGAGAAGCAGCAG-GAACCAG-3′) were used for hamster PGAP3, and 5′-GCTGTCCCTGTAT-GCCTCTGG-3′ and 5′-TCTCGGCTGTGGTGGTGAAG-3′ were used for β-actin as internal control. The data were analyzed by SDS2 software (Applied Biosystems), and each standard curve was automatically produced whose R2 values of β-actin, primer set A and B were 0.989, 0988, and 0.995, respectively. The amounts of PGAP3 mRNA were normalized by β-actin and those of GD3S-C37 were set as ratio = 1. PGAP3 cDNA containing full-length of coding region was amplified from DM2&3-C2 RNA by Phusion DNA polymerase (Finnzymes, Espoo, Finland) with primers 5′-AGTGCAACATGAA-CACAGATACTTCC3′ and 5′GTGAGAGCCAGCAAGGGGT3′ and subcloned into pBluescriptII vector. The sequence of six independent clones revealed that two of six clones had 19 base pairs insertion (TCCTGTCTGTCT-GTTTCAG) between 60th and 61th amino acids. To examine whether this insertion was specific to DM2&3-C2 cells, the region of 190 base pairs containing this site from both GD3S-C37 and DM2&3-C2 RNAs was amplified by PCR (35 cycles) with primer set A (see above) and amplified DNA fragments were applied to 3% agarose gel.

Fluorescence-activated Cell Sorting (FACS) Analysis

Cells (5×10^6) were suspended in 0.4 ml of Opti-MEM I (Invitrogen) with 20–25 μg of the indicated plasmids and electroporated at 260 V and 1000 μF by using a Gene Pulser (Bio-Rad). Two days after transfection, cells were stained with antibodies against CD59 or uPAR and PE-conjugated goat anti-mouse IgG and analyzed by FACS Caliber (BD Biosciences).

Establishing Mutant Cells

C84 and AM-B cells were treated with 0.24 mg/ml ethyl methanesulfonate (EMS) for 24 h, cultured for 1 wk, and CD59-positive cells were enriched twice by auto MACS (Miltenyi Biotec, Auburn, CA) with biotinylated 5H8 anti-CD59 and streptavidin microbeads and sorted in FACS Vantage after staining with 5H8 anti-CD59 and PE-conjugated anti-mouse IgG, and limiting-diluted to obtained clones. The majority of cloned cell lines were double mutants of PGAP1 and PGAP2. DM1&2-C14 and -C17 were obtained from AM-B and C84 cells, respectively. To obtain double-mutant cells of PGAP2 and PGAP3, sorted CD59-positive cells were treated with PI-PLC, and PI-PLC–sensitive cells were collected and limiting diluted. DM2&3-C2 was established from C84 cells.

Purification of PI from Surface GPI-APs

About 2×10^9 cells, expressing HFGF-CD59, were suspended in 12 ml of buffer A [9.6% (wt/vol) sucrose, 20 mM HEPES-NaOH, pH 7.4, and protease inhibitors (10 μg/ml leupeptin, 10 μg/ml aprotinin, and 1 mM phenylmethylsulfonyl fluoride)], destroyed by nitrogen cavitation (PARR Instrument, Moline, IL) (300 psi at 4°C for 20 min) and centrifuged at $10,000 \times g$ at 4°C for 10 min. The supernatant was transferred to a new tube. The pellet was resuspended in 6 ml of buffer A, destroyed again by nitrogen cavitation (300 psi at 4°C for 15 min) and centrifuged. The supernatant was saved. Finally, the pellet was resuspended in 2 ml of buffer A, passed through a 22-gauge needle 10 times, and centrifuged again. All supernatants were combined (~18 ml in total), and 1.5 ml each of the combined supernatant was placed on each of 10 ml of a continuous sucrose gradient (20–50%, wt/vol) in 20 mM HEPES-NaOH, pH 7.4, prepared in 12 tubes by Gradient Master (BioComp Systems, Minneapolis, MN). After ultracentrifugation at 35,000 rpm (SW41 rotor) at 4°C for 16–18 h, fractions of 1 ml were collected from the top using Piston Gradient Fractionator (BioComp Systems). Aliquots of each fraction were applied to SDS-polyacrylamide gel electrophoresis (PAGE)/Western blotting with antibodies against CD59, transferrin receptor (TfR), syntaxin6, and ribophorins II to determine fractions containing the plasma membrane without contaminating ER membrane. Typically, fractions 2–6 (total 60 ml from 12 tubes) were used for further steps. These combined fractions were divided into six tubes for SW28 rotor and mixed with 27 ml of chilled 20 mM HEPES-NaOH, pH 7.4, per tube. After ultracentrifugation at 25,000 rpm (SW28 rotor) at 4°C for 16–18 h, the pellets were suspended in total 11 ml of Tris-buffered saline-E (TBS-E) (20 mM Tris-Cl, pH 7.4, 150 mM NaCl, and 1 mM EDTA) containing 60 mM 1-octyl-β-D-glucoside and protease inhibitors, and lysed for 2 h at 4°C. After ultracentrifugation at 28,000 rpm (SW41 rotor) at 4°C for 1 h, the supernatant was transferred to a new tube and incubated with 100 μl of bed volume of glutathione beads overnight. The glutathione (GSH) beads were washed with 1 ml of TBS-E containing 60 mM 1-octyl-β-D-glucoside twice followed by 1 ml of TBS-E containing 1% Triton X (TX)-100 three times. The binding proteins were eluted four times after 5-min incubation on ice with 200 μl each of elution buffer (20 mM GSH, 30 mM Tris-Cl, and 1% TX-100 in TBS-E). All eluates were combined, mixed with 14 μl of 10% deoxycholate and 80 μl of trichloroacetic acid (TCA), incubated on ice for 30 min, and centrifuged at 4°C for 20 min. The pellet was washed with 1 ml of ethanol twice, air-dried, resuspended in 200 μl of 2× sample buffer, applied to SDS-PAGE, and transferred to polyvinylidene difluoride (PVDF) membrane. PI was purified from PVDF membrane, as described previously (Fontaine *et al.*, 2003). PVDF membrane was stained with 0.1% Ponceau S in 5% acetic acid, and the band corresponding to HFGF-CD59 was cut, washed with water four times, and incubated with a mixture of 500 μl of 0.3 M NaOAc, pH 4.0, buffer and 500 μl of freshly dissolved 1 M sodium nitrite for 3 h at 37°C. After washing the PVDF membrane strips with 1 ml of water four times, PI was extracted in 400 μl of butan-1-ol saturated with water three times. The extracted PI in butan-1-ol was dried up under N_2 stream, dissolved in 200 μl of chloroform/methanol 4:1 (C/M 4:1), and immediately applied to a column (200-μl bed) of Si60 silica (Sigma-Aldrich) packed in a glass Pasteur pipette plugged with glass wool and prewashed with 1 ml of C/M 1:4 three times followed by 1 ml of C/M 4:1 three times. After washing the column with 0.4 ml of C/M 4:1 five times, PI was eluted with 0.2 ml of C/M 1:4 five times, dried up under N_2 stream, and redissolved in 100 μl of C/M 2:3 for mass spectrometry.

Electrospray Ionization Mass Spectrometric (ESI-MS) Analysis of Phospholipids

The ESI-MS analyses were performed using a 4000Q TRAP, quadrupole-linear ion trap hybrid MS (Applied Biosystems/MDS Sciex, Foster City, CA) with a LC-10AD VP high-performance liquid chromatography system combined with SIL-10AD VP autosampler (Shimadzu, Kyoto, Japan). Phospholipids were subjected directly to ESI-MS analysis without LC separation by flow injection; typically, 4 μl of sample was applied. The mobile phase composition was acetonitrile/methanol/water (6:7:2) (plus 0.1% ammonium formate) at a flow-rate of 8 μl/min. The scan range of the instrument was set at m/z 400–950 at a scan speed of 1000 Da/s. The trap fill-time was set at 3 ms in the positive ion mode and at 5 ms in the negative ion mode. The ion spray voltage was set at 5500 V in the positive ion mode and at −4500 V in the negative ion mode. Neutral loss scanning of 277 Da (phosphorylinositol + NH_4) was used for the detection of positive-molecular-weight–related ions of PI (M + NH_4) and precursor ion scanning of m/z 241 (phosphorylinositol − H_2O) was used for the detection of negative-molecular-weight–related ions of PI (M − H) (Taguchi *et al.*, 2005). Nitrogen was used as curtain gas (setting of 10, arbitrary units) and as collision gas (set to "high"). The declustering potential was set at 20 V to minimize in-source fragmentation. The enhanced product ion scanning used at collision energy of −55 eV in the negative ion mode. Q1 resolution was set to high, and Q3 resolution was set to unit mass. Collision energy of the neutral loss scanning was set at 25 to 40 eV in the positive ion mode.

Immunofluorescence Microscopy

CHO cells transfected with pME-PGAP3/PERLD1-3HA by using Lipofectamine 2000 (Invitrogen) were fixed with 4% paraformaldehyde in PBS for 20 min at room temperature. After quenching with 40 mM ammonium chloride in PBS, the cells were permeabilized with PBS containing 0.1% TX-100 and 2.5% goat serum for 1 h at room temperature and stained with rabbit anti-GPP130 and mouse anti-HA antibodies followed by Alexa 594-conjugated goat anti-rabbit IgG and Alexa 488-conjugated goat anti-mouse IgG antibodies. The pictures were taken by BX50 microscope (Olympus, Tokyo, Japan) and VB-6010 charge-coupled device (CCD) camera (Keyence, Osaka, Japan).

Detergent-resistant Membrane (DRM) Fractionation

Cells were detached from the plate by using PBS containing 2.5 mM EDTA and 0.5% bovine serum albumin. After centrifugation, the cell pellet was resuspended in MBS-E [25 mM 2-(*N*-morpholino)ethanesulfonic acid, pH 6.5, 150 mM NaCl, and 5 mM EDTA] containing protease inhibitors supplemented with 1% TX-100, incubated for 20 min on ice, and homogenized by a potter-type Teflon homogenizer. The volume of lysis buffer was ~20 times the weight of cell pellet (typically 25–30 million cells/ml lysis buffer). One milliliter of lysate was mixed with 1 ml of 80% (wt/vol) sucrose in MBS-E, transferred to a centrifuge tube for SW41, overlaid with 7 ml of 30% and 2 ml of 5% sucrose in MBS-E, ultracentrifuged at 38,000 rpm for 16–18 h at 4°C, and

A

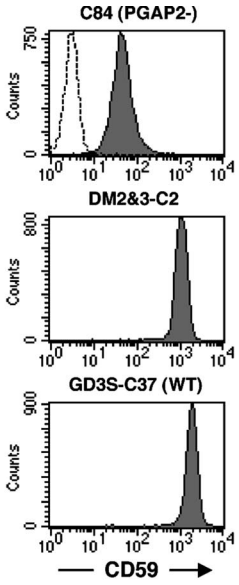

C

3B2A(WT)		DM2&3-C2	
MS	MS/MS	MS	MS/MS
alk 34:0	16:0-18:0	alk 34:1	16:0-18:1
acyl 34:0	16:0-18:0	acyl 34:1	16:0-18:1
alk 36:1	18:1-18:0	alk 36:1	18:0-18:1
alk 36:0	18:0-18:0	alk 38:4	18:0-20:4 16:0-22:4
acyl 36:0	18:0-18:0	acyl 38:4	18:0-20:4

B

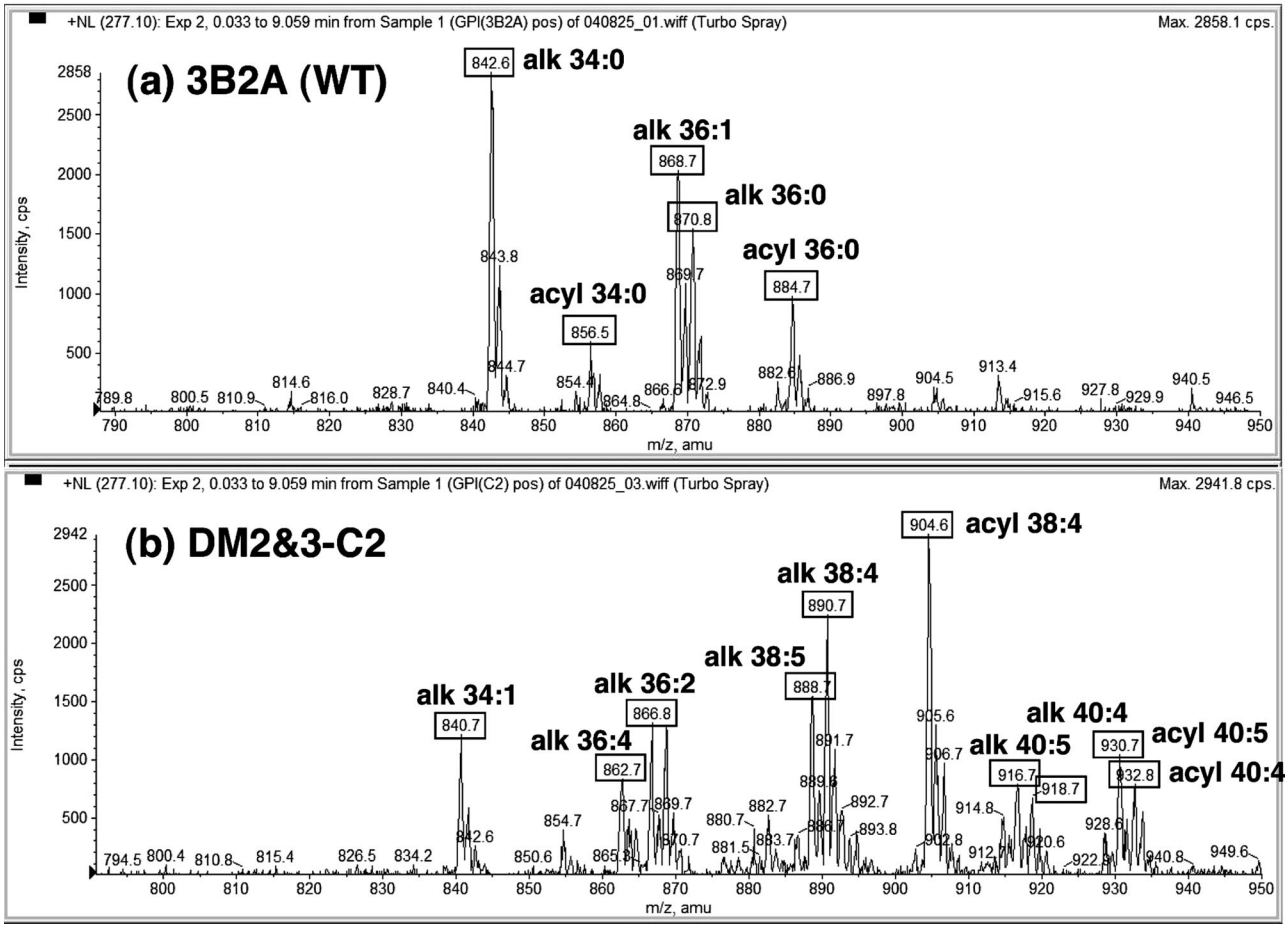

Figure 1. PGAP2&3 double-mutant cells are defective in fatty acid remodeling of GPI-APs. (A) Restored surface expression of CD59 on double-mutant DM2&3-C2 cells derived from C84 PGAP2-deficient cells. C84 PGAP2-single-mutant (parent for DM2&3-C2; top), DM2&3-C2 double-mutant (middle), and GD3S-C37 wild-type (parent for C84; bottom) cells were stained with antibody 5H8 against human CD59 and analyzed by FACS. A dotted line in C84 cells represents background staining without anti-CD59 antibody. (B) MS analysis of PI of epitope-tagged CD59 isolated from the plasma membrane. Top (A) and bottom (B), wild-type 3B2A and DM2&3-C2 cells, respectively. Alk and acyl represent alkyl-acyl (or alkenyl-acyl) and diacyl glycerols, respectively, and figures before and after colon represent the number of total carbons and unsaturated bonds, respectively. Neutral loss scanning of 277 Da (phosphorylinositol + NH_4) was used for the detection of positive molecular weight-related ions. (C) Summary of the MS/MS analysis (Supplemental Figure S1) of various precursor PI species of

fractionated from the top using Piston Gradient Fractionator (BioComp Systems) with each fraction of 1 ml (total 11 fractions). Fractions 2–4, 5–8, and 9–11 were combined as top, middle, and bottom fractions, respectively. Aliquots of each fraction were mixed with 6× sample buffer, without a reducing reagent, and applied to 4–20% gradient SDS-PAGE.

Fractionation of GPI-APs with Octyl-Sepharose

3B2A, C10 (PGAP1 single-deficient), and DM1&2-C17 (PGAP1 and PGAP2 double-mutant) cells (5×10^7) were transfected with pME-Neo2dH-VSVGts-FF-mEGFP-GPI (Tashima *et al.*, 2006). Cells were cultured for half a day at 37°C followed by 1.5 d at 32°C and harvested. The cell pellets were lysed in 5 ml of lysis buffer (60 mM 1-octyl-β-D-glucoside and protease inhibitors in TBS-E) for 1 h at 4°C. After centrifugation at 15,000 rpm at 4°C for 15 min, the supernatants were incubated with M2 anti-FLAG beads overnight. The immunoprecipitates were washed twice with 0.5 ml of buffer (30 mM 1-octyl-β-D-glucoside in TBS-E), twice with 0.5 ml of buffer (20 mM Tris-HCl, pH 7.4, and 0.1% Nonidet P-40), and twice with 0.5 ml of buffer (20 mM Tris-HCl, pH 7.4, and 0.03% Nonidet P-40). FLAG-mEGFP-GPI was eluted with 100 μl of 0.1 M ammonium acetate containing 1 mg/ml FLAG-peptide (Sigma-Aldrich) and 0.03% Nonidet P-40 four times (total volume 400 μl). One hundred microliters of the eluate was mixed with 100 μl of buffer (0.1 M ammonium acetate, 0.03% Nonidet P-40, and 10% 1-propanol), loaded onto an octyl-FF column (GE Healthcare), and chromatographed in ÄKTA (GE Healthcare) at a flow rate of 0.5 ml/min by using a 5–40% gradient of 1-propanol. Fractions of 0.7 ml were collected, dried, and subjected to SDS-PAGE/Western blotting by using M2 antibody against FLAG-tag followed by HRP-conjugated anti-mouse IgG antibody.

RESULTS

PGAP2 and PGAP3 Double-Mutant Cells Are Defective in Fatty Acid Remodeling of GPI-APs

After a new round of mutagenesis of PGAP2 single-mutant CHO cells with ethylmethane sulfonate, we obtained cells with restored GPI-APs expression, such as CD59, DAF (CD55), and uPAR, and termed one clone of the double-mutant cell, DM2&3-C2 (Figure 1A). We termed the gene defective in DM2&3-C2 as PGAP3. Using this double-mutant and wild-type 3B2A cells, we compared the composition of PI moiety of the surface GPI-APs. For this, we established cells with stable expression of epitope-tagged CD59, HFGF-CD59. HFGF-CD59 was extracted from the plasma membrane, purified with glutathione-beads, applied to SDS-PAGE, transferred to PVDF membrane, and subjected to sodium nitrite treatment to release PI from GPI by means of deamination of glucosamine residue (Fontaine *et al.*, 2003). The released PI was analyzed by MS in positive ion mode with neutral loss scanning of 277 Da (phosphorylinositol + NH_4). The patterns of m/z peaks were quite different between wild-type and DM2&3-C2 cells: the majority of released PIs from HFGF-CD59 of wild-type cells had only saturated fatty chains, whereas the majority of released PIs from HFGF-CD59 of DM2&3-C2 had unsaturated chains (Figure 1B). To determine which of the two fatty chains, sn-1– or sn-2–linked, is unsaturated, we performed MS/MS analysis of five precursor PI species separated in the first negative ion mode MS (precursor ion scanning of m/z 241) (Supplemental Figure S1). The MS/MS analysis of the five precursor PI species from wild-type cells separated in the MS revealed that stearic acid (C18:0) was exclusively used at sn-2 position, whereas in DM2&3-C2 cells oleic (C18:1), arachidonic (C20:4), and docosatetraenoic (C22:4) acids were used at sn-2 (Figure 1C), indicating that GPI-APs undergo the fatty acid remodeling in that unsaturated chain at sn-2 is replaced by saturated stearoyl chain.

Figure 1 (cont). epitope-tagged CD59 detected in the first negative ion mode MS (precursor ion scanning of m/z 241). Stearic acid (C18:0) was exclusively used at sn-2 position of PI in wild-type cells (left), whereas oleic (18:1), arachidonic (20:4) and docosatetraenoic (C22:4) acids were used at the same position in DM2&3-C2 cells (right). Alkyl chains are underlined.

Fatty Acid Remodeling Is Critical for the Raft Association of GPI-APs

It is thought that saturated fatty chains in GPI-APs are important for integration into the liquid-ordered raft membrane (Schroeder *et al.*, 1994; Melkonian *et al.*, 1999; Moffett *et al.*, 2000; Zhang *et al.*, 2000; Raza Shaikh *et al.*, 2003). However, clear experimental evidence has not been presented, because GPI-APs with unsaturated fatty chains at sn-2 position are rare in the plasma membrane of normal cells, except for GPI-APs with inositol-linked fatty acid (Roberts *et al.*, 1988; Redman *et al.*, 1994; Brewis *et al.*, 1995; Treumann *et al.*, 1995; Benting *et al.*, 1999). As DM2&3-C2 cells expressed GPI-APs with unsaturated fatty chains, they are useful to assess requirement of the saturated chains for raft association of GPI-APs. Through this study, we defined raft association as partitioning into DRMs, which is the sole biochemical method widely used and accepted; yet, we noticed that DRM can be somewhat different from physiologically relevant lipid rafts (Lichtenberg *et al.*, 2005). We examined whether CD59, uPAR and DAF were fractionated into DRM by sucrose density gradient ultracentrifugation, after solubilization with 1% TX-100 (Figure 2A) (Brown and Rose, 1992). Caveolin-1 and flotillin-1, and TfR were used as raft and nonraft markers, respectively. These markers (flotillin-1 not shown) were similarly fractionated in both wild-type GD3S-C37 and DM2&3-C2 cells. In wild-type cells, most of the GPI-APs were present in the DRM fractions (U), whereas in DM2&3-C2 cells <20% of GPI-APs were in the DRM fraction (Figure 2B). The differences between wild-type and double-mutant cells were statistically significant (two-sided p value = 0.0004 for DAF, 0.0002 for uPAR and <0.0001 for CD59 by t test). These results clearly indicated that the saturated lipid chain at sn-2 is critical for the raft association of GPI-APs.

PGAP3, the Gene Responsible for the Second Defect in DM2&3-C2, Encodes a Protein Mainly Expressed in the Golgi

Some of us recently showed that yeast PER1 (Ng *et al.*, 2000) is involved in lipid remodeling of GPI-APs, and we identified per1-like domain containing 1 (PERLD1) as the mammalian homologue (Fujita *et al.*, 2006a). Mammalian PERLD1 encodes a protein of 320 amino acids, which has 28% identity with yeast PER1. Transfection of either human PERLD1 or yeast PER1 decreased the surface expression of CD59 and uPAR on DM2&3-C2 to the levels on PGAP2 single-mutant cells (Figure 3A), indicating that PERLD1 was the PGAP3. The expression of PGAP3/PERLD1 together with PGAP2 in DM2&3-C2 restored the association of GPI-APs with lipid rafts (Figure 3, B and C), indicating that the weak association of GPI-APs with lipid rafts in DM2&3-C2 was in fact due to a lack of fatty acid remodeling.

To confirm that PGAP3 is the gene mutated in DM2&3-C2 double-mutant cells, we first cloned the normal Chinese hamster PGAP3 cDNA and sequenced it (GenBank accession no. AB288236). Hamster PGAP3 encodes a protein of 320 amino acids, which has 86, 91, and 91% identities with human, mouse, and rat PGAP3, respectively. Based on the sequence, we performed real-time RT-PCR by using two different sets of primers to evaluate the amount of PGAP3 transcript in the double-mutant cells. After normalization by β-actin as an internal control, the amount of PGAP3 transcript in DM2&3-C2 was assessed to be <20% of that in GD3S-C37 (Figure 3D). By sequencing full-length RT-PCR

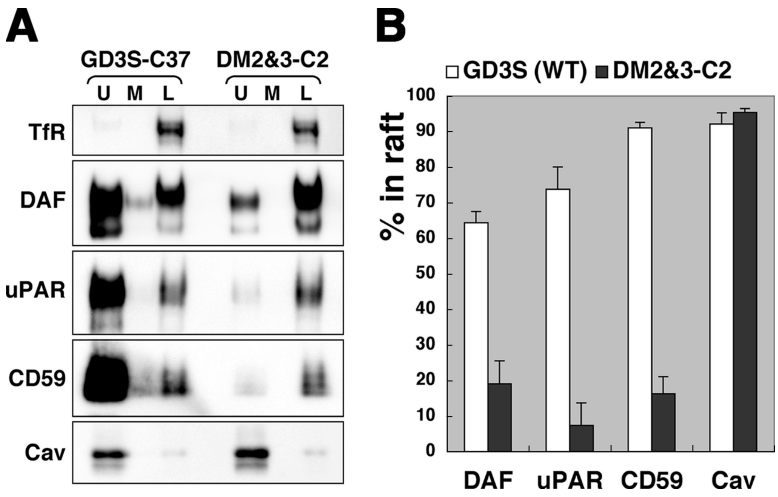

Figure 2. Fatty acid remodeling is critical for the raft association of GPI-APs. (A) Proteins in wild-type GD3S-C37 and DM2&3-C2 cells were fractionated by sucrose density gradient ultracentrifugation after solubilization in 1% TX-100 at 4°C. Aliquots of top (U), middle (M), and bottom (L) fractions after ultracentrifugation were analyzed by SDS-PAGE/Western blotting with antibodies against TfR, DAF, uPAR, CD59, and caveolin-1 (Cav). U and L correspond to raft (detergent-resistant) and nonraft (detergent-soluble) fractions, respectively. This picture is representative of three independent experiments. (B) Amounts of DAF, uPAR, CD59, and Cav in U and L fractions were measured on Western blots with a CCD camera, and the percentage of proteins in the raft was calculated as the ratio of intensity in L to that of U+L fractions. Results are means and standard deviations from three independent experiments.

products, we found a 19-base pair insertion (TCCTGTCT-GTCTGTTTCAG) after the 60th amino acid that caused frame shift followed by appearance of immature stop codon closely downstream of this site. The last 15 base pairs of this insertion were almost the same as sequence of mouse PGAP3 intron 1 acceptor site (GTTTGTCTGTTTCAG; Evidence Viewer, National Center for Biotechnology Information, Bethesda, MD), indicating the presence of splicing defect between exons 1 and 2. Moreover, we detected other minor but abnormal PGAP3 transcripts in DM2&3-C2 by RT-PCR around exons 1 and 2 junction with primer set A, which may reflect aberrant splicing (Figure 3E, asterisks). Thus, these results indicated that PGAP3 was the gene responsible for the second mutation.

Immunofluorescent microscopic analysis of HA-tagged PGAP3 expressed in CHO cells revealed its main localization in the Golgi with weaker staining of punctate unidentified organelle and the ER (Figure 3F). Together with the previous report that PGAP2 is localized mainly to the Golgi (Tashima *et al*., 2006), it is suggested that the fatty acid remodeling most likely occurs in the Golgi. This is in contrast to two other examples of fatty acid remodeling of GPI known to occur in the ER in bloodstream form of *T. brucei* (Morita *et al*., 2000) and *S. cerevisiae* (Sipos *et al*., 1997; Bosson *et al*., 2006). Two proteins, Per1p (Fujita *et al*., 2006a) and Gup1p (Sipos *et al*., 1997; Bosson *et al*., 2006), in yeast, which are involved in removal of sn-2 chain and incorporation of C26:0 chain, respectively, are localized to the ER.

A Defect in PGAP1 Inhibits Fatty Acid Remodeling Mediated by PGAP3 and PGAP2

We also obtained a different kind of double-mutant cell line with restored surface expression of GPI-APs from C84 and another line from PGAP2-deficient AM-B cells (Tashima *et al*., 2006). We found that the surface GPI-APs on these double-mutant cells were resistant to PI-PLC (Figure 4Ad), indicating that the PGAP1 gene (Tanaka *et al*., 2004) was defective, in addition to PGAP2. Moreover, these double-mutant clones, termed DM1&2-C14 and -C17 (data not shown), became like a PGAP2-single mutant after transfection of PGAP1 (Figure 4Ae). PGAP1 is the inositol-deacylase that removes palmitic acid linked to inositol in GPI before GPI-APs exit from the ER (Tanaka *et al*., 2004). The palmitoylated inositol renders GPI-APs resistant to PI-PLC. That the defect in PGAP1 restored the surface expression of GPI-APs indicated either that elimination of palmitic acid from inositol is required for the subsequent removal of unsaturated sn-2 chain (three lipid chains remained); that removal of sn-2 chain occurs, but the presence of inositol-linked palmitoyl chain inhibited the action of the PLD that cleaves off the proteins (two lipid chains remained); or that PLD cleaves GPI, but the proteins are still attached to the membrane via palmitic acid (one lipid chain remained). To determine the number of chains linked to GPI-APs in DM1&2-C17 cells, we used hydrophobic chromatography with octyl-Sepharose, with which lyso GPI-AP (one lipid chain) was nicely separated from two-lipid-chain GPI-AP (Tashima *et al*., 2006). With a gradient concentration of 1-propanol, FLAG-mEGFP-GPI, a model GPI-AP from DM1&2-C17 cells, was reproducibly eluted in fractions 16–20 (Figure 4Bc) like three-chained FLAG-mEGFP-GPI from PGAP1-deficient cells (Figure 4Bb), whereas the same GPI-APs from wild-type cells bearing two lipid chains was eluted earlier in fractions 15–18 (Figure 4Ba), indicating that surface GPI-APs expressed on DM1&2-C17 had three lipid chains. Our attempt to directly analyze the lipid moiety by liquid chromatography-MS/MS has not been successful due to inability to recover inositol-acylated PI after nitrous acid deamination of GPI-AP. There are reports that inositol-acylated acetylcholine esterase (Roberts *et al*., 1988) and CD59 from human erythrocytes (Rudd *et al*., 1997), and CD52 from spleen cells (Treumann *et al*., 1995) had a highly unsaturated fatty acid at sn-2 position. Together, we conclude that inositol-deacylation is an essential step in fatty acid remodeling.

DISCUSSION

In this article, we report several new findings: 1) replacement of unsaturated fatty chain at sn-2 with saturated stearic acid in GPI-APs, fatty acid remodeling, occurs in mammalian cells; 2) PGAP2 and PGAP3 are involved in this process; 3) fatty acid remodeling is critical for the integration of GPI-APs into lipid rafts; and 4) inositol-deacylation by PGAP1 is an essential step in fatty acid remodeling. Figure 5 is a schematic of the current model of fatty acid remodeling of mammalian GPI-APs.

The modification of proteins by GPI is observed in eukaryotes from yeast to mammals and also plants (McConville and Ferguson, 1993; Ferguson, 1999; Ikezawa, 2002). GPI-APs are synthesized in the ER, transported to the plasma membrane via the secretory pathway through the Golgi, and incorporated into specialized microdomains, so-called lipid

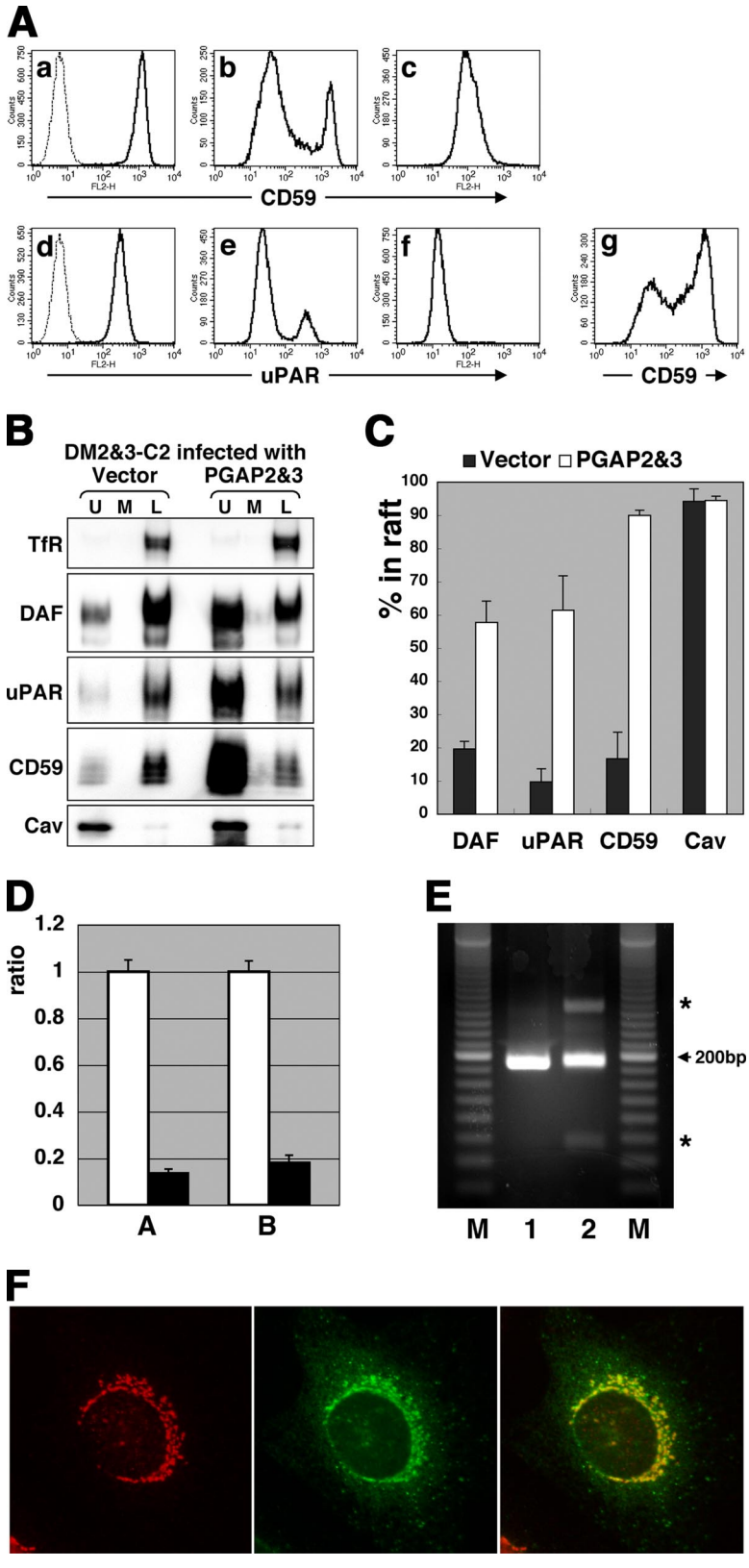

Figure 3. PGAP3, the gene responsible for the second defect in DM2&3-C2, encodes a protein mainly expressed in the Golgi. (A) FACS analysis of the surface expression of CD59 (a–c and g) and uPAR (d–f) on DM2&3-C2 cells transiently transfected with control (a and d), human PGAP3 (b and e), or yeast PER1 (g) expression vector and on C84 PGAP2-single-mutant cells transfected with control vector (c and f). Dotted lines (a and d) represent background staining without antibodies. (B) Proteins in DM2&3-C2 cells stably transfected with PGAP2 and PGAP3 were fractionated as described in Figure 2. Fractions obtained from two independent experiments showed a quite similar pattern to fractions obtained from wild-type cells, as shown in Figure 2. (C) The percentages of proteins in rafts were quantified as described in Figure 2. Results are means and standard deviations from two independent experiments. (D) The amounts of PGAP3 mRNA expressed in GD3S-C37 (white bars) and DM2&3-C2 (black bars) were evaluated by real-time RT-PCR. Two different primer sets (set A, left and set B, right) were used for PCR of PGAP3, and the amount was normalized by the amount of β-actin. The relative ratio was calculated with the amount in GD3S-C37 being set as 1. Bars represent SD of n = 3. (E) PGAP3 cDNAs obtained from GD3S-C37 (lane 1) and DM2&3-C2 (lane 2) were amplified by PCR with primer set A. Twenty base-pair ladder maker DNA was used as reference (lanes M). Asterisks, two abnormal bands in lane 2. (F) Expression of PGAP3 in the Golgi. DM2&3-C2 cells transiently transfected with HA-tagged PGAP3 were fixed, permeabilized with TX-100, and stained for GPP130, a Golgi protein, (left) and HA (middle). (Right) Merged profile showing colocalization of GPP130 and PGAP3.

rafts (Brown and Rose, 1992; Simons and Ikonen, 1997). The raft association is major and a common characteristic of GPI-APs in mammalian cells, and it is related to functions of GPI-APs in various ways. Cross-linking of GPI-APs or the ligand binding evokes the activation or association of Src-type nonreceptor tyrosine kinases (Shenoy-Scaria *et al.*, 1992; Tansey *et al.*, 2000). Folate receptor, a GPI-AP, is endocytosed via unique compartments, GPI-AP enriched early en-

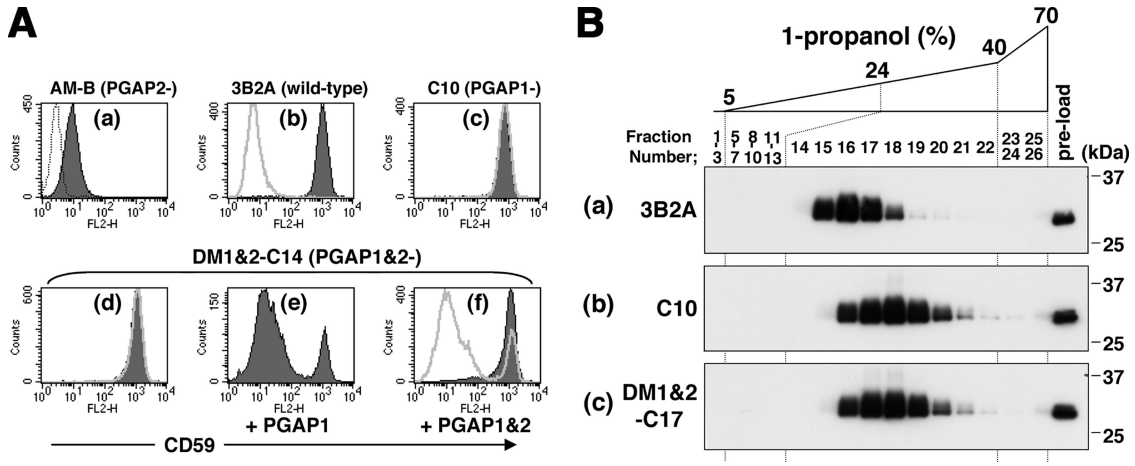

Figure 4. A defect in PGAP1 inhibits fatty acid remodeling mediated by PGAP3 and PGAP2. (A) Surface expression of CD59 was examined by FACS in AM-B, another PGAP2-single-mutant (a), wild-type 3B2A (b), C10 PGAP1-single mutant (c), and DM1&2-C14 (d–f) cells. DM1&2-C14 cells were either nontransfected (d), transiently transfected with PGAP1 expression vector (e), or cotransfected with PGAP1 and PGAP2 expression vectors (f). A dotted line (a) represents background staining. Thick gray lines (b–d and f) indicate the cells treated with PI-PLC. (B) 3B2A wild-type, C10 PGAP1-single-mutant, and DM1&2-C17 cells were transiently transfected with VSVGts-FF-mEGFP-GPI expression vector and the processed FLAG-mEGFP-GPI was collected from the cell lysates with anti-FLAG beads and eluted with a FLAG-peptide (Tashima *et al*., 2006). FLAG-mEGFP-GPIs were chromatographed in an octyl-FF column with a 5–40% gradient of 1-propanol. Fractions were subjected to SDS-PAGE and analyzed by Western blotting with an anti-FLAG antibody.

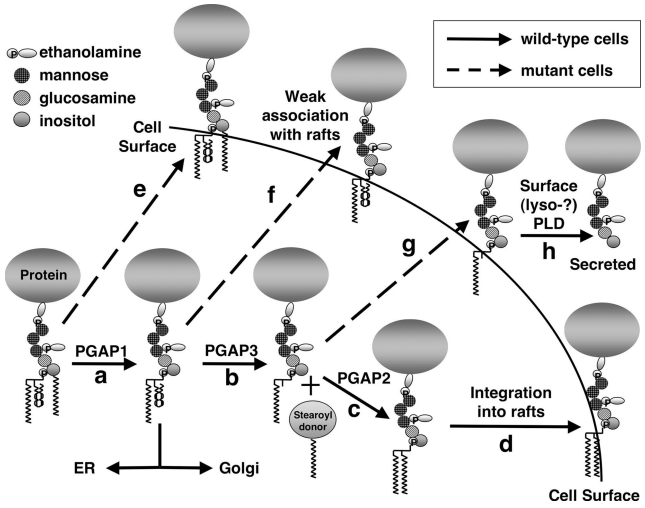

Figure 5. Current model of fatty acid remodeling of GPI-APs in mammalian cells. GPI is synthesized from PI with an unsaturated fatty acid at sn-2 position and has an acylated (usually palmitoylated) inositol. Immediately after attachment of GPI to newly synthesized proteins, inositol-linked palmitate is removed by PGAP1, the deacylase, in the ER (step a). The inositol-deacylation is essential for subsequent steps in fatty acid remodeling in the Golgi. An unsaturated fatty chain at sn-2 is removed, resulting in lyso-GPI-APs. PGAP3 is involved in this step (step b). Reacylation of sn-2 with stearic acid follows and PGAP2 is involved in this step (step c). A donor of stearoyl chain is yet to be determined. GPI-APs that have undergone fatty acid remodeling are competent for the integration into lipid rafts (step d). In PGAP1-deficient cells, GPI-APs before inositol deacylation are expressed on the cell surface without any further modification (step e). In PGAP3-deficient cells, GPI-APs carrying an unsaturated fatty chain at sn-2 are expressed on the cell surface (step f). In PGAP2-deficient cells, lyso-form GPI-APs are transported to the cell surface (step g), rapidly cleaved by surface (lyso-) PLD, and secreted (step h). PGAP1, PGAP3, and PGAP2 are epistatic in this order.

dosome compartments (Sabharanjak *et al*., 2002), and the replacement of GPI with transmembrane and cytoplasmic portions of low-density lipoprotein receptor causes much less efficient uptake of 5-methyl tetrahydrofolate (Ritter *et al*., 1995). The compartmentalization of ephrin-A, a GPI-anchored ligand, is essential for the normal response of growth cone to its receptor, EphA (Marquardt *et al*., 2005). GPI-APs are selectively transported to apical surface in polarized cells (Brown and Rose, 1992). Although these characteristics are thought to be dependent upon their raft association, little is known about how GPI-APs are associated with lipid rafts. From the studies of raft-associated phospholipids (Schroeder *et al*., 1994; Raza Shaikh *et al*., 2003) and palmitoylated proteins (Melkonian *et al*., 1999; Moffett *et al*., 2000; Zhang *et al*., 2000), straight acyl chains are strongly proposed to be important for their raft integrations. The present study showed for the first time that it is also true for GPI-APs, because GPI-APs with unsaturated fatty chains brought by the defect of the remodeling were associated with lipid rafts much weaker than normal rafts. Association of GPI-APs with lipid rafts was assessed by their recovery into DRM after sucrose density gradient centrifugation. Clearly, fatty chains are major determinants for DRM association of GPI-APs. Whether the decreased DRM association of unremodeled GPI-APs has any effect in various functions of GPI-APs discussed above is very interesting and is now experimentally testable.

Recent several reports, including the present report, have revealed components and their functions in the lipid remodeling in yeast and mammalian cells. There are similarity and difference between two systems. First, homologous components are used. PGAP3 in mammalian system and PER1p (Fujita *et al*., 2006a) in yeast are involved in generation of lyso-GPI-APs. PGAP3 and PER1p are functionally interchangeable between both species. PGAP3 does not have a lipase-like motif but has several serine and histidine residues that are conserved in active sites of PLA_2 family (Fujita *et al*., 2006a). It is clear that PGAP3 is required for PLA_2 activity; however, we still do not know whether PGAP3 is an

enzyme itself or a factor that regulates the enzyme activity. A sequence homologue of PGAP2 (Tashima *et al*., 2006) in yeast is CWH43p (Martin-Yken *et al*., 2001). The yeast mutant cwh43-2, originally isolated for its Calcofluor White hypersensitivity, shows several cell wall defects, which notably include increased release of Cwp1p, a GPI-AP (Martin-Yken *et al*., 2001) as seen in our PGAP2-deficient CHO cells (Tashima *et al*., 2006). Because many GPI-APs, such as Cwp1p, Cwp2p, Gas1p, and Dcw1p, are involved in yeast cell wall biogenesis (Kitagaki *et al*., 2002), we assume that such cell wall defects are caused by aberrant biogenesis of GPI-APs due to defective remodeling, although precise involvement of CWH43p is yet to be determined. PGAP2 does not have any known motif or domain, and its precise function is currently under investigation. PGAP1 (Tanaka *et al*., 2004) and the yeast homologue Bst1p (Fujita *et al*., 2006b) are deacylases of an acyl chain linked to inositol of GPI in the ER, and they are required for subsequent remodeling in both species. Yeast Gup1p belongs to membrane-bound *O*-acyl transferase family and is required for the addition of C26 fatty chain to the sn-2 position (Bosson *et al*., 2006). Although mammalian acyltransferase for the remodeling has not been identified, several mammalian proteins belong to this family, and one of them may function in the remodeling.

Second, both systems use the particular fatty acid for the replacement, i.e., C18:0 fatty acid in CHO cells and C26:0 in yeast, indicating that acyltransferases have narrow substrate specificities, yet the possibility that only particular lipids are available in the lumen of the ER/Golgi has not been excluded.

Third, in CHO cells the remodeling is thought to take place mainly in the Golgi, based on the localization of PGAP2 (Tashima *et al*., 2006) and PGAP3, although we cannot exclude the possibility that it dose occur in the ER, whereas in yeast the ER is the main site of the remodeling (Bosson *et al*., 2006; Fujita *et al*., 2006b). Although determination of PI structure in mammalian GPI-APs still in the ER is necessary for more precise localization of the site of the remodeling, it is not practical at the moment to collect an enough amount of ER-form of GPI-APs for lipid chain analysis. It is interesting to notice that the integration of GPI-APs into rafts also takes place in the same compartments where GPI-APs undergo the remodeling, the ER in yeast (Bagnat *et al*., 2000) and the Golgi in mammals (Brown and Rose, 1992). The observation that GPI-APs before the remodeling associate very weakly with rafts puts a concern about the theory that lipid rafts are formed in the Golgi in mammalian cells, because the theory is based upon both the fact that GPI-APs become competent for the recovery into detergent resistant membranes in the Golgi during their transports and an assumption that GPI-APs are always integrated into rafts if rafts are present there. Now, we have another possibility that lipid rafts are formed in earlier organelles such as ER, but that only GPI-APs that undergo the remodeling in the Golgi are able to associate with rafts. Our separate study demonstrated that GPI-APs expressed in PGAP1 mutants have considerable affinity for lipid rafts, although weaker, compared with those expressed in wild-type cells, as judged by conventional DRM fractionation method (Maeda and Kinoshita, unpublished observation). As the lipid structure of GPI-APs in PGAP1 mutant cells are unchanged through all the way from the ER to the cell surface, PGAP1 mutant cells will be useful to reevaluate where lipid rafts are formed.

Fourth, the transport of Gas1p from the ER to the Golgi was substantially delayed in per1-deleted yeast (Ng *et al*., 2000; Fujita *et al*., 2006b), whereas we did not observe significant transport delay of GPI-APs from the ER to the surface in CHO DM2&3-C2 cells (Maeda and Kinoshita, our unpublished observation). It is suggested that the raft association may be required for the efficient exit from the ER in yeast but may not be required for exit from the Golgi in mammalian cells. Because the defect of either PGAP1 (Tanaka *et al*., 2004) or Bst1p (Elrod-Erickson and Kaiser, 1996; Fujita *et al*., 2006b) similarly caused the delayed transport of GPI-APs from the ER to the Golgi, the ER may more strictly regulate the sorting to exit site or transport vesicles than the Golgi.

GPI-APs on human erythrocytes, such as acetylcholine esterase (Roberts *et al*., 1988) and CD59 (Rudd *et al*., 1997), and CD52 on a population of spleen cells (Treumann *et al*., 1995), maintain inositol-linked palmitate on the cell surface, presumably due to an insufficient activity of PGAP1. Interestingly, such GPI-APs had a highly unsaturated lipid chain at the sn-2 position, indicating that fatty acid remodeling was also affected in these molecules. The results obtained from the analysis of PGAP1&2 double-mutant cells in this study was compatible with these known GPI structures, indicating that inositol deacylation by PGAP1 is an essential step in fatty acid remodeling.

Finally, raft disrupting reagents have been commonly used to study biological significance of the raft association of GPI-APs, but such reagents may exert side effects. Genetic manipulation of fatty acid remodeling should be useful in studying the function of rafts on sorting of and signaling from GPI-APs.

ACKNOWLEDGMENTS

We thank F. Mori and K. Kinoshita for excellent technical assistance, and K. Nakamura for help with cell sorting. We also thank M. A. Ferguson for helpful discussions and technical advice on PI purification and Y. Horiguchi and S. Kamitani for help and guidance in chromatography. This work was supported by grants from Mizutani Foundation; the Ministry of Education, Culture, Sports, Science and Technology of Japan; and the Core Research for Evolutional Science and Technology, Japan Science and Technology Agency.

REFERENCES

Bagnat, M., Keranen, S., Shevchenko, A., Shevchenko, A., and Simons, K. (2000). Lipid rafts function in biosynthetic delivery of proteins to the cell surface in yeast. Proc. Natl. Acad. Sci. USA *97*, 3254–3259.

Benting, J., Rietveld, A., Ansorge, I., and Simons, K. (1999). Acyl and alkyl chain length of GPI-anchors is critical for raft association in vitro. FEBS Lett. *462*, 47–50.

Bosson, R., Jaquenoud, M., and Conzelmann, A. (2006). GUP1 of *Saccharomyces cerevisiae* encodes an O-acyltransferase involved in remodeling of the GPI anchor. Mol. Biol. Cell *17*, 2636–2645.

Brewis, I. A., Ferguson, M. A., Mehlert, A., Turner, A. J., and Hooper, N. M. (1995). Structures of the glycosyl-phosphatidylinositol anchors of porcine and human renal membrane dipeptidase. Comprehensive structural studies on the porcine anchor and interspecies comparison of the glycan core structures. J. Biol. Chem. *270*, 22946–22956.

Brown, D. A., and Rose, J. K. (1992). Sorting of GPI-anchored proteins to glycolipid-enriched membrane subdomains during transport to the apical cell surface. Cell *68*, 533–544.

Elrod-Erickson, M. J., and Kaiser, C. A. (1996). Genes that control the fidelity of endoplasmic reticulum to Golgi transport identified as suppressors of vesicle budding mutations. Mol. Biol. Cell *7*, 1043–1058.

Ferguson, M. A. (1999). The structure, biosynthesis and functions of glycosylphosphatidylinositol anchors, and the contributions of trypanosome research. J. Cell Sci. *112*, 2799–2809.

Fontaine, T., Magnin, T., Melhert, A., Lamont, D., Latge, J. P., and Ferguson, M. A. (2003). Structures of the glycosylphosphatidylinositol membrane anchors from Aspergillus fumigatus membrane proteins. Glycobiology *13*, 169–177.

Fujita, M., Umemura, M., Yoko-o, T., and Jigami, Y. (2006a). PER1 is required for GPI-phospholipase A2 activity and involved in lipid remodeling of GPI-anchored proteins. Mol. Biol. Cell *17*, 5253–5264.

Fujita, M., Yoko, O. T., and Jigami, Y. (2006b). Inositol deacylation by Bst1p is required for the quality control of glycosylphosphatidylinositol-anchored proteins. Mol. Biol. Cell *17*, 834–850.

Hancock, J. F. (2006). Lipid rafts: contentious only from simplistic standpoints. Nat. Rev. Mol. Cell Biol. *7*, 456–462.

Harder, T., and Simons, K. (1997). Caveolae, DIGs, and the dynamics of sphingolipid-cholesterol microdomains. Curr. Opin. Cell Biol. *9*, 534–542.

Ikezawa, H. (2002). Glycosylphosphatidylinositol (GPI)-anchored proteins. Biol. Pharm. Bull. *25*, 409–417.

Kerwin, J. L., Tuininga, A. R., and Ericsson, L. H. (1994). Identification of molecular species of glycerophospholipids and sphingomyelin using electrospray mass spectrometry. J. Lipid Res. *35*, 1102–1114.

Kitagaki, H., Wu, H., Shimoi, H., and Ito, K. (2002). Two homologous genes, DCW1 (YKL046c) and DFG5, are essential for cell growth and encode glycosylphosphatidylinositol (GPI)-anchored membrane proteins required for cell wall biogenesis in *Saccharomyces cerevisiae*. Mol. Microbiol. *46*, 1011–1022.

Lichtenberg, D., Goni, F. M., and Heerklotz, H. (2005). Detergent-resistant membranes should not be identified with membrane rafts. Trends Biochem. Sci. *30*, 430–436.

Marquardt, T., Shirasaki, R., Ghosh, S., Andrews, S. E., Carter, N., Hunter, T., and Pfaff, S. L. (2005). Coexpressed EphA receptors and ephrin-A ligands mediate opposing actions on growth cone navigation from distinct membrane domains. Cell *121*, 127–139.

Martin-Yken, H., Dagkessamanskaia, A., De Groot, P., Ram, A., Klis, F., and Francois, J. (2001). *Saccharomyces cerevisiae* YCRO17c/CWH43 encodes a putative sensor/transporter protein upstream of the BCK2 branch of the PKC1-dependent cell wall integrity pathway. Yeast *18*, 827–840.

McConville, M. J., and Ferguson, M. A. (1993). The structure, biosynthesis and function of glycosylated phosphatidylinositols in the parasitic protozoa and higher eukaryotes. Biochem. J. *294*, 305–324.

Melkonian, K. A., Ostermeyer, A. G., Chen, J. Z., Roth, M. G., and Brown, D. A. (1999). Role of lipid modifications in targeting proteins to detergent-resistant membrane rafts. Many raft proteins are acylated, while few are prenylated. J. Biol. Chem. *274*, 3910–3917.

Moffett, S., Brown, D. A., and Linder, M. E. (2000). Lipid-dependent targeting of G proteins into rafts. J. Biol. Chem. *275*, 2191–2198.

Morita, Y. S., Paul, K. S., and Englund, P. T. (2000). Specialized fatty acid synthesis in African trypanosomes: myristate for GPI anchors. Science *288*, 140–143.

Ng, D. T., Spear, E. D., and Walter, P. (2000). The unfolded protein response regulates multiple aspects of secretory and membrane protein biogenesis and endoplasmic reticulum quality control. J. Cell Biol. *150*, 77–88.

Paladino, S., Sarnataro, D., Pillich, R., Tivodar, S., Nitsch, L., and Zurzolo, C. (2004). Protein oligomerization modulates raft partitioning and apical sorting of GPI-anchored proteins. J. Cell Biol. *167*, 699–709.

Raza Shaikh, S., Dumaual, A. C., LoCassio, D., Siddiqui, R. A., and Stillwell, W. (2003). Acyl chain unsaturation in PEs modulates phase separation from lipid raft molecules. Biochem. Biophys. Res. Commun. *311*, 793–796.

Redman, C. A., Thomas-Oates, J. E., Ogata, S., Ikehara, Y., and Ferguson, M. A. (1994). Structure of the glycosylphosphatidylinositol membrane anchor of human placental alkaline phosphatase. Biochem. J. *302*, 861–865.

Ritter, T. E., Fajardo, O., Matsue, H., Anderson, R. G., and Lacey, S. W. (1995). Folate receptors targeted to clathrin-coated pits cannot regulate vitamin uptake. Proc. Natl. Acad. Sci. USA *92*, 3824–3828.

Roberts, W. L., Myher, J. J., Kuksis, A., Low, M. G., and Rosenberry, T. L. (1988). Lipid analysis of the glycoinositol phospholipid membrane anchor of human erythrocyte acetylcholinesterase. Palmitoylation of inositol results in resistance to phosphatidylinositol-specific phospholipase C. J. Biol. Chem. *263*, 18766–18775.

Rudd, P. M., Morgan, B. P., Wormald, M. R., Harvey, D. J., van den Berg, C. W., Davis, S. J., Ferguson, M. A., and Dwek, R. A. (1997). The glycosylation of the complement regulatory protein, human erythrocyte CD59. J. Biol. Chem. *272*, 7229–7244.

Sabharanjak, S., Sharma, P., Parton, R. G., and Mayor, S. (2002). GPI-anchored proteins are delivered to recycling endosomes via a distinct cdc42-regulated, clathrin-independent pinocytic pathway. Dev. Cell *2*, 411–423.

Schroeder, R., London, E., and Brown, D. (1994). Interactions between saturated acyl chains confer detergent resistance on lipids and glycosylphosphatidylinositol (GPI)-anchored proteins: GPI-anchored proteins in liposomes and cells show similar behavior. Proc. Natl. Acad. Sci. USA *91*, 12130–12134.

Shenoy-Scaria, A. M., Kwong, J., Fujita, T., Olszowy, M. W., Shaw, A. S., and Lublin, D. M. (1992). Signal transduction through decay-accelerating factor. Interaction of glycosyl-phophatidylinositol anchor and protein tyrosine kinases p56lck and p59fyn1. J. Immunol. *149*, 3535–3541.

Simons, K., and Ikonen, E. (1997). Functional rafts in cell membranes. Nature *387*, 569–572.

Simons, K., and Toomre, D. (2000). Lipid rafts and signal transduction. Nat. Rev. Mol. Cell Biol. *1*, 31–39.

Sipos, G., Reggiori, F., Vionnet, C., and Conzelmann, A. (1997). Alternative lipid remodelling pathways for glycosylphosphatidylinositol membrane anchors in *Saccharomyces cerevisiae*. EMBO J. *16*, 3494–3505.

Taguchi, R., Houjou, T., Nakanishi, H., Yamazaki, T., Ishida, M., Imagawa, M., and Shimizu, T. (2005). Focused lipidomics by tandem mass spectrometry. J. Chromatogr. B. Analyt. Technol. Biomed. Life Sci. *823*, 26–36.

Tanaka, S., Maeda, Y., Tashima, Y., and Kinoshita, T. (2004). Inositol deacylation of glycosylphosphatidylinositol-anchored proteins is mediated by mammalian PGAP1 and yeast Bst1p. J. Biol. Chem. *279*, 14256–14263.

Tansey, M. G., Baloh, R. H., Milbrandt, J., and Johnson, E. M., Jr. (2000). GFRalpha-mediated localization of RET to lipid rafts is required for effective downstream signaling, differentiation, and neuronal survival. Neuron *25*, 611–623.

Tashima, Y., Taguchi, R., Murata, C., Ashida, H., Kinoshita, T., and Maeda, Y. (2006). PGAP2 is essential for correct processing and stable expression of GPI-anchored proteins. Mol. Biol. Cell *17*, 1410–1420.

Treumann, A., Lifely, M. R., Schneider, P., and Ferguson, M. A. (1995). Primary structure of CD52. J. Biol. Chem. *270*, 6088–6099.

Wong, Y. W., and Low, M. G. (1992). Phospholipase resistance of the glycosylphosphatidylinositol membrane anchor on human alkaline phosphatase. Clin. Chem. *38*, 2517–2525.

Zhang, J., Pekosz, A., and Lamb, R. A. (2000). Influenza virus assembly and lipid raft microdomains: a role for the cytoplasmic tails of the spike glycoproteins. J. Virol. *74*, 4634–4644.